Catalytic Activity of Oxygen Carriers on the Removal of Tar Byproducts for Biomass Chemical Looping Gasification Application

energy&fuels

pubs.acs.org/EF

Article

Catalytic Activity of Oxygen Carriers on the Removal of Tar Byproducts for Biomass Chemical Looping Gasification Application

Iván Samprón, Victor Purnomo, Tobias Mattisson, Henrik Leion, Luis F. de Diego, and Francisco García-Labiano*

Cite This: *Energy Fuels* 2023, 37, 16629–16638

Read Online

ACCESS | Metrics & More | Article Recommendations

ABSTRACT: One of the main advantages of chemical looping gasification (CLG) in comparison to conventional gasification technologies is its potential to enhance in situ tar removal. This is due to the catalytic properties of the oxygen carrier used in the CLG process, which can facilitate tar oxidation, cracking, and reforming reactions under specific operating conditions. Furthermore, this catalytic effect can be harnessed to convert hydrocarbons (C_1–C_3), thereby increasing syngas production during the process. In this study, the catalytic activity of eight different oxygen carriers (two ores, two wastes, and four synthetic materials) was examined in a batch fluidized bed reactor. The reactions were mainly conducted at three temperatures (850, 900, and 950 °C), utilizing benzene and ethylene as model compounds. The results revealed that the ores and wastes exhibited a low catalytic effect over benzene and ethylene conversion at low temperatures, although this effect was increased with a rising temperature. Conversely, the synthetic materials demonstrated higher catalytic activity in the benzene and ethylene conversion reactions, which also increased with higher temperatures. It should be noted that the Cu/Al oxygen carrier achieved nearly complete conversion of benzene and ethylene at temperatures exceeding 900 °C. Methane production was observed in most of the experiments, indicating its role as an intermediate in the conversion of tar byproducts. Additionally, the Cu/Al oxygen carrier exhibited a promising catalytic performance in methane conversion. These findings highlight the potential of certain synthetic oxygen carriers, such as the Cu/Al oxygen carrier, to serve as effective catalysts for the removal of tar byproducts and light hydrocarbons during CLG processes.

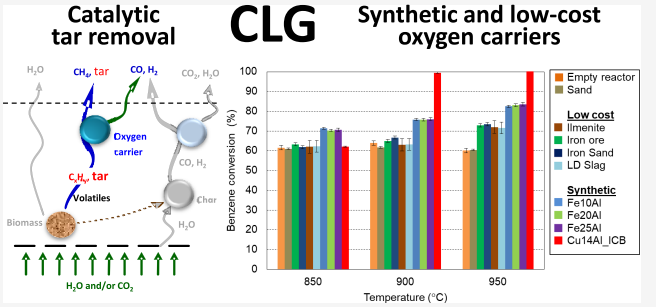

1. INTRODUCTION

Biomass chemical looping gasification (BCLG) has emerged in recent years as a promising energy conversion technology that enables the production of renewable syngas. BCLG is performed in two interconnected fluidized bed reactors: an air reactor (AR), where oxidation of an oxygen carrier takes place, and a fuel reactor (FR), where fuel conversion occurs. The solid oxygen carrier is used as bed material to transport oxygen between reactors, being oxidized and reduced in the separate reactors.[1] Since the oxygen carrier transfers only oxygen from the air reactor to the fuel reactor, N_2 dilution of syngas, which is typical of conventional gasification processes, and the need for expensive pure gaseous O_2 are avoided. In addition, CO_2 generated in biomass gasification is concentrated in the fuel reactor. This can lead to negative carbon emissions if the CO_2 is separated from the syngas and sent for storage. The syngas generated in the gasification process has many possible uses, ranging from a direct utilization in a gas turbine to further processing steps to obtain valuable products like chemicals or liquid biofuels.[2]

Chemical looping technologies, especially chemical looping combustion (CLC), have been intensively studied in the past 20 years.[3] For this reason, in the literature, a wide range of oxygen carriers were proposed for CLC, and many of them have been tested in continuous operation units.[4] There are also several studies about oxygen carrier development for the BCLG process, but in this case, only a few of them have been carried out in continuous operation units ranging from 1.5 to 25 kW_{th}.[5−16] Investigation in continuous operation units is important since the high reducing environment in BCLG may cause agglomeration or defluidization of the oxygen carrier bed, or decreased reactivity of the oxygen carrier itself.[17,18] Apart from investigations of oxygen carrier performance, recent studies on BCLG have addressed the effort to improve syngas

Received: July 24, 2023
Revised: September 26, 2023
Published: October 11, 2023

https://doi.org/10.1021/acs.energyfuels.3c02750
Energy Fuels 2023, 37, 16629−16638

yield and gas quality through reforming of the generated hydrocarbons and removal of pollutants.[19−22] The removal of tars is necessary, as they can cause issues like catalyst deactivation, corrosion, and plugging of pipelines.[23,24] Moreover, some tar substances are harmful for health and environment.[25]

There are various definitions of tar in the scientific community. According to Devi et al.,[24] tar consists of condensable hydrocarbons from single to 5-aromatic rings, oxygen-containing compounds, and complex polycyclic aromatic hydrocarbons (PAHs). Meanwhile, Torres et al.[26] stated that tars roughly comprise organic compounds produced from thermal decomposition from biomass or organic materials, as well as from partial oxidation of fuels. Since tar may have a complex composition, its structure is determined by multiple factors, such as the properties of fuel used and the operating temperature of the gasifier.[24,27] The latter determines which tar compounds would be formed, as different compounds have different dew points; see Figure 1.

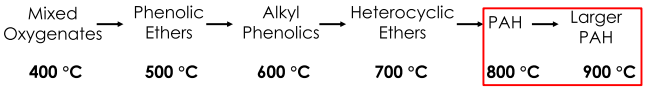

Figure 1. Tar maturation as a function of the dew point. Adapted from Elliot.[28]

Figure 1 shows that most aromatic tar compounds are formed at temperatures higher than 800 °C, which are the typical temperatures in BCLG. Previous studies reported that naphthalene, anthracene, biphenyl, phenanthrene, acenaphthylene, and benzene are the most common compounds formed in such process.[6,7,10−12] In general, aromatic tar compounds have high stability and are difficult to break down into lighter products without using catalysts. Beyond widely known high-temperature tar cracking,[29] hot catalytic tar removal has been highlighted as a promising strategy since it can be performed in the first steps of gasification.[30,31] This would be effective as a method to avoid problems in downstream processes, corrosion in the unit, and fouling and plugging of the pipelines.

Previous studies have reported tar byproduct concentrations of ∼150 g/Nm^3 in biomass gasification when it was carried out in updraft fixed or spouted beds and ∼40 g/Nm^3 when it was carried out in fluidized beds using inert bed material.[32] Compared to these numbers, the use of catalysts in fluidized beds was demonstrated to reduce the content of tar byproducts by half, with respect to the use of inert materials.[33,34] Thus, apart from transferring oxygen from air to fuel reactor, which enables tar combustion, oxygen carriers in BCLG can improve tar conversion into lighter products through catalytic cracking.[31] Although it does occur, the combustion of tar byproducts is less likely during gasification due to the substoichiometric conditions, which provides an oxygen carrier in the fuel reactor that is mostly reduced with little available lattice oxygen.[6] Therefore, it is necessary to study the catalytic properties of oxygen carriers under reduced conditions for screening purposes prior to their use in BCLG.

Some authors have investigated the catalytic effect of oxygen carriers using tar subrogates, such as ethylene and benzene.[35,36] These studies found a catalytic effect on benzene conversion using La, Sr, and Fe in ZrO_2-based oxygen carriers, but the mentioned solids have never been used in BLCG continuous operation due to their low mechanical stability under reducing conditions.[35] In addition, recent advances in BCLG have shown a wide range of suitable oxygen carriers that were not considered previously for the process. This includes synthetic oxygen carriers, wastes, and ores.

The aim of this work was to investigate in a batch fluidized bed reactor the catalytic activity of eight oxygen carriers on the removal of tar byproducts under typical BCLG conditions. Ethylene and benzene were used as substitute compounds to emulate tar byproducts of different weights. Ethylene was used due to the similarity of its bonds to those present in aromatic tar byproducts.[37] Benzene was chosen since it is one of the most difficult hydrocarbons to crack, hence providing the worst-case scenario.[35] The results obtained were compared with data available in the literature from the continuous operation of BCLG prototypes.

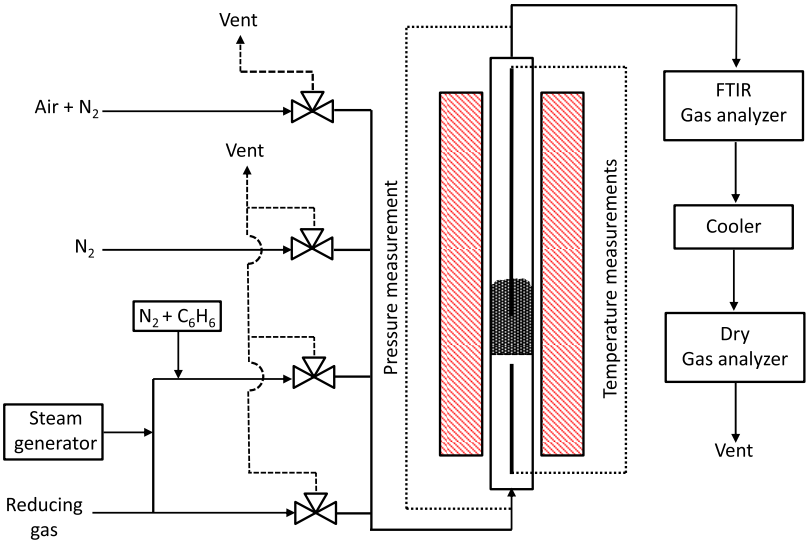

Figure 2. Schematic layout of the batch fluidized bed.

https://doi.org/10.1021/acs.energyfuels.3c02750
Energy Fuels 2023, 37, 16629−16638

2. MATERIALS AND METHODS

2.1. Batch Fluidized Bed Reactor. The experiments were carried out in a quartz glass batch fluidized bed reactor (i.d., 22 mm), which was placed inside an electrically heated furnace. The main scheme of the system is shown in Figure 2. Further information could be found elsewhere.[38]

The temperature was measured using two K-type thermocouples enclosed in the reactor, and the pressure drop was measured by 20-Hz pressure transducers. Reduction and oxidation reactions taking place in a continuous operation were emulated by feeding 1 Nl/min of reducing and oxidizing gases alternatively with an inert stage between them to flush the reactor with nitrogen gas. The reducing gas (free of N_2) comprised 37.2 vol % steam, 26.1 vol % CO, 9.1 vol % CO_2, 14 vol % H_2, 8.5 vol % CH_4, and 3 vol % C_2H_4. The remaining 2.1 vol % corresponded to C_6H_6. Benzene was introduced by saturating a 0.3 Nl/min N_2 stream that passed through a vessel containing liquid benzene at a controlled temperature system set at 6 °C. Therefore, the stream fed to the fluidized bed reactor accurately emulates the typical environment taking place in the fuel reactor of a BLCG system in continuous operation. Nitrogen-depleted air (5 vol % O_2) was used as oxidizing gas to avoid a high-temperature rise in the reactor and therefore the agglomeration of the oxygen carrier. The concentrations of steam, ethylene, and benzene were measured by a Thermo-Scientific iS50 FTIR spectrometer. The concentrations of CO, CO_2, H_2, CH_4 (dry basis), and O_2 in the outlet gas were continuously measured by a Rosemount NGA 2000 gas analyzer.

2.2. Oxygen Carriers. Eight oxygen carriers were used: two ores, two waste-based materials, and four synthetic solids. The ores consisted of a hematite from Tierga (Spain) composed of 76.5 wt % of Fe_2O_3 and an ilmenite provided by the company Titania S/A (Norway), which is used for titanium production. These materials have commonly been used in chemical looping processes due to their low cost and abundance.[6,9,12,16] The waste-based materials were a copper slag provided by Boliden AB, also known as iron sand, which was recently proposed for the CLG process,[39] and the steel processing residue LD slag, which has been used previously both in the CLC and CLG processes.[8,40] Three synthetic oxygen carriers contained 10, 20, and 25 wt % of Fe_2O_3 on alumina (Fe10Al, Fe20Al, and Fe25Al), and the other one was composed of 14 wt % of CuO on alumina (Cu14Al_ICB). Before being used, all the materials were calcined for 2 h in an air atmosphere in a muffle furnace to increase their mechanical strength. Further information about the preparation of these materials could be found elsewhere.[10,11] The calcination temperature of the materials was 950 °C, except for the Cu14Al_ICB oxygen carrier, which was calcined at 850 °C as in a previous study.[41] The oxygen carriers were characterized by several techniques. A Bruker D8 Advance A25 polycrystalline powder X-ray diffractometer was used to determine the crystalline phases. The metal content of the oxygen carriers was determined by inductively coupled plasma-optical emission spectroscopy (ICP-OES) using an Xpectroblue-EOP-TI FMT26 (Spectro) spectrophotometer. A Micromeritics AccuPyc II 1340 helium pycnometer was used to measure the skeletal density. Crushing strength was determined by the average of 20 measurements in a Shimpo FGN-5X digital force gauge. The BET surface area was measured using an ASAP2020 instrument from Microactive software. Mercury intrusion measured by a Quantachrome PoreMaster 133 instrument was used to determine the porosity of the particles.

The oxygen carrier transport capacity, R_{OC}, was defined as the maximum mass fraction of the oxygen carrier that can be used for oxygen transfer. This was determined in a CI Electronics TGA, following the procedure described in a previous study.[25] A mixture of 15 vol % CO and 20 vol % CO_2 (N_2 balance) was used as a reducing agent and air for oxidation. CO was used instead of H_2 as a reducing agent because previous studies showed that CO was capable of completely reducing $Fe_2O_3{\cdot}Al_2O_3$ to $FeAl_2O_4$.[42,43] The main properties of the fresh calcined oxygen carriers are shown in Table 1.

2.3. Experimental Procedure. The experimental procedure followed in this work was intended to emulate the typical fluidization behavior and operation conditions taking place in the fuel reactor of a

Table 1. Main Physical and Chemical Properties of the Fresh Oxygen Carriers

	ores		wastes		synthetic			
	ilmenite	iron ore	iron sand	LD slag	Fe10Al	Fe20Al	Fe25Al	Cu14Al_ICB
particle size (μm)	100−300	100−300	100−180	100−300	100−300	100−300	100−300	100−300
skeletal density (kg/m^3)	4100	4216	3410	2764	3744	3950	4105	3699
crushing strength (N)	2.2 ± 0.4	5.8 ± 1.7	1.4 ± 0.6	3.7 ± 1.0	1.8 ± 0.6	1.5 ± 0.6	1.6 ± 0.4	1.5 ± 0.5
porosity (%)	1.2	26.3	17.2	14.1	50.2	45.6	44.4	50.0
BET (m^2/g)	<1	1.4	<1	2.7	60.9	37.7	19.7	79.4
oxygen transport capacity, Roc	0.043	0.077	0.010	0.018	0.010	0.020	0.025	0.029
main XRD phases	Fe_2TiO_5 (54.7 wt %)	Fe_2O_3 (76.5 wt %)	Fe_2O_3 (57.8 wt %)	CaO	Fe_2O_3	Fe_2O_3	Fe_2O_3	CuO
	Fe_2O_3 (11.2 wt %)	SiO_2	Fe_3O_4 (31.3 wt %)	Ca_2SiO_4	α-Al_2O_3	α-Al_2O_3	α-Al_2O_3	$CuAl_2O_4$
	TiO_2 (28.6 wt %)	Al_2O_3	SiO_2	$Ca_2Fe_2O_5$	θ-Al_2O_3	θ-Al_2O_3	θ-Al_2O_3	α-Al_2O_3
		CaO		$Mg_2Fe_2Si_2O_5$				δ-Al_2O_3
		MgO		$CaMn_{14}SiO_{24}$				
				$Ca_3Mg(SiO_4)_2$				
				Mg_2SiO_4				

https://doi.org/10.1021/acs.energyfuels.3c02750
Energy Fuels 2023, 37, 16629−16638

BCLG continuous unit. Thus, for each experimental test, 15 g of bed material was loaded on the distribution plate of the reactor and subsequently heated under a nitrogen atmosphere up to 850 °C. Each oxygen carrier was exposed to activation steps by performing redox cycles using the same gas composition and flow rates as those used later in the experimental tests. This was done before the BCLG experiments in order to ensure stable fuel conversion. Once stabilized, the oxygen carrier was reduced for 1000 s with the aforementioned gas concentrations, keeping the temperature at 850 °C. After the reducing step, a flow of N_2 was passed for 300 s to remove the remaining gases in the system. Then, the oxygen carrier was oxidized for 1200 s with 5 vol % O_2. After that, the temperature was raised first to 900 °C and later to 950 °C, and the process was repeated again in the same way at 850 °C. For each oxygen carrier, at least two cycles were performed at three different temperatures (850, 900, and 950 °C) with the same batch of bed particles in the reactor. All experiments were repeated twice to ensure repeatability. In the last redox cycle carried out at 950 °C, the test was stopped after the reduction stage and the reactor was cooled in a N_2 atmosphere to determine the reduced crystalline phases of the oxygen carrier. Additional tests, following the same procedure, were carried out with the Cu14Al_ICB oxygen carrier in a wide range of temperatures (750, 800, 850, 860, 870, 880, 890, 900, and 950 °C) to obtain detailed information about the temperature effect on the catalytic activity of this oxygen carrier.

The conversion of hydrocarbons, X_{CxHy} (%), was calculated as the molar fraction of the hydrocarbon at the outlet of the reactor with respect to the amount fed to the inlet, as expressed in eq 1.

$$X_{CxHy}\,(\%) = \frac{x_{CxHy,in} \times Q_{in} - x_{CxHy,out} \times Q_{out}}{x_{CxHy,in} \times Q_{in}} \times 100 \quad (1)$$

where Q_{in} and Q_{out} are the inlet and the outlet gas flow rates (mol/h) in the reactor, whereas $x_{CxHy,in}$ and $x_{CxHy,out}$ are the fractions of hydrocarbons analyzed at the inlet and outlet gas streams, respectively. The conversions were calculated in the steady or pseudosteady state (plateaus such as those in Figure 3) and were average conversions during the steady or pseudosteady state.

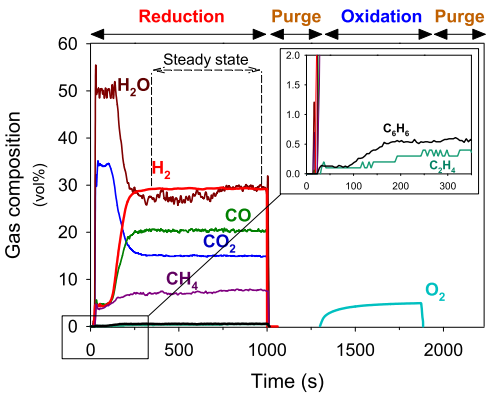

Figure 3. Outlet gas concentration profile in a redox cycle using ilmenite as the oxygen carrier at 850 °C. The steady state is remarked.

3. RESULTS AND DISCUSSION

A typical profile of the gas outlet composition during a complete redox cycle, using ilmenite at a temperature of 850 °C, is shown in Figure 3. Similar profiles were obtained at other temperatures and with other oxygen carriers. During the first seconds of reaction in the reduction stage, a peak of CO_2 and H_2O was observed as a consequence of the high level of lattice oxygen present in the oxygen carrier in its initial state. Smaller amounts of H_2, CO, and CH_4 were also detected due to the incomplete combustion of these reducing gases. It is noteworthy that the reaction between the oxygen carrier and the gas phase was carried out mainly with CO and H_2, whereas CH_4 was only slightly converted due to its lower reactivity. Likewise, the lattice oxygen converted some of the C_2H_4 and C_6H_6, although both compounds were detected at the outlet of the reactor in the reduction period.

After the initial approximate 50 s of oxygen carrier reduction, the availability of lattice oxygen decreased and caused a decline in the concentrations of CO_2 and H_2O, whereas the other compounds showed the opposite trend. This involved the end of the combustion stage and the maximum possible reduction of the oxygen carrier to its lowest oxidation state allowed by thermodynamic or kinetic limitations. At this point, the gas concentrations stabilized, indicating that a steady or pseudosteady state had been reached. These steady or pseudosteady state conditions allowed for the evaluation of the catalytic effect of the reduced oxygen carrier operating under gasification conditions in the fuel reactor, without taking into account the contribution due to oxidation. It should be noted that oxygen mass balances were carried out in several of the redox cycles, and the difference between the oxygen transferred by the oxygen carrier and that calculated according to the oxygen transport capacity of Table 1 was within the experimental error of ±10%.

3.1. Crystalline Phase Characterization. As mentioned above, the oxygen carriers in BCLG can act as catalysts for several tar removal reactions, making BCLG more advantageous compared with other conventional gasification technologies. In general, it is known that metallic phases (Ni^0, Cu^0, and Fe^0) have a greater catalytic effect than their oxidized phases (metal oxides) and are responsible for the catalysis of several reactions.[44,45] However, fully reduced metallic phases may not be achieved in BCLG due to thermodynamic or kinetic constraints. For this reason, it is important to determine the stable phases reached by the oxygen carriers under gasification conditions. In this work, the crystalline phases that formed in reduced samples were characterized by XRD, after being removed from the reactor at the end of the test. Figure 4 shows the diffractograms of reduced samples of both synthetic and low-cost materials (ores and wastes) used in the experiments.

As can be seen in Figure 4a, the phases formed in the synthetic Fe/Al oxygen carriers under reducing gasification conditions were free Al_2O_3 and $FeAl_2O_4$. This is reasonable since the presence of steam and CO_2 prevents further reduction of both metal oxides to metallic compounds, with aluminate being the only Fe-based stable species.[42,43,46] In contrast, the Cu-based synthetic material, Cu14Al_ICB, was reduced to metallic copper under the same operating conditions. In the temperature range used in this work, this reduction pathway is maintained regardless of the temperature at which the tests are performed.[11]

Both natural ores (ilmenite and iron ore) and wastes (iron sand and LD slag) were characterized by the presence of several phases of Fe-oxides that involve elements such as Ca and Si (Figure 4b). The main phases formed in the reduced ilmenite were $FeTiO_3$ and Fe_3O_4, as well as minor amounts of TiO_2. The reduced iron ore was composed of different iron oxides, such as Fe_3O_4, FeO, and other mixed compounds, i.e., $Fe_2Ca_2O_5$. Minor amounts of SiO_2, typical of ore materials, were also found. In addition to iron oxides, different phases comprising Ca and Si were also found in the waste materials.

https://doi.org/10.1021/acs.energyfuels.3c02750
Energy Fuels 2023, 37, 16629−16638

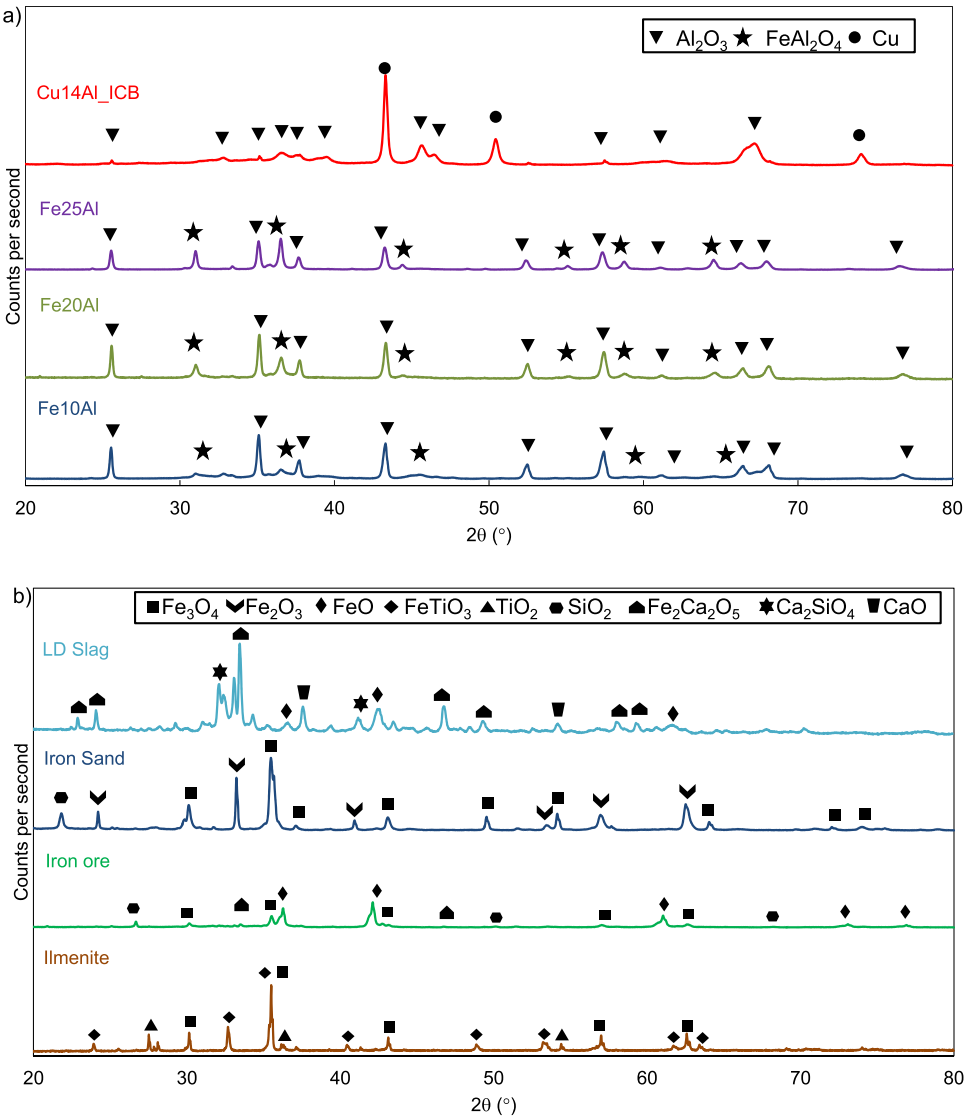

Figure 4. Diffractograms of the reduced samples once the steady state was achieved during the reduction period of (a) synthetic oxygen carriers and (b) ore- and waste-based materials after the 950 °C redox cycles.

The iron sand waste was mainly composed of Fe_2O_3 and Fe_3O_4, whereas smaller amounts of SiO_2 were also detected. The steel production residue LD slag was reduced to different Fe and Ca oxides (FeO, CaO, and Ca_2SiO_4) and $Fe_2Ca_2O_5$, as seen in Figure 4b.

3.2. Catalytic Effect of Oxygen Carriers on the Conversion of Hydrocarbons. The catalytic activity of the aforementioned oxygen carriers on the removal of tar byproducts was studied in a batch fluidized bed reactor. In order to evaluate the catalytic effect separately from other conversion routes, additional experiments were done by using (i) no bed material (empty reactor) and (ii) sand as bed material.

3.2.1. Ethylene Conversion. Figure 5 shows the C_2H_4 conversion reached with the reduced materials in a steady or pseudosteady state at three different temperatures. The catalytic activity of oxygen carriers on the hydrocarbon conversion differs depending on temperature and the type of oxygen carrier. At 850 °C, the ethylene conversion, when using ores and wastes as the oxygen carriers, was similar to that obtained in the experiment carried out with a sand bed (X_{C2H4}

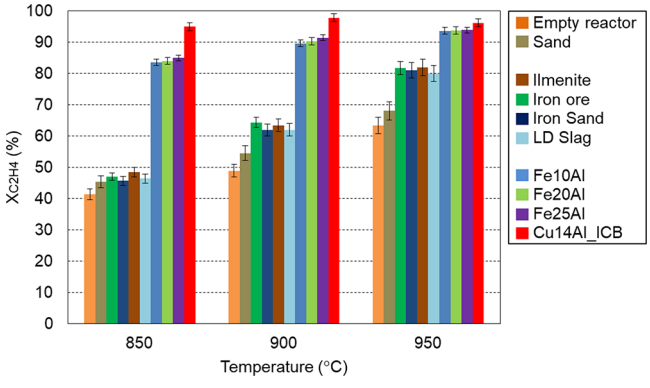

Figure 5. Ethylene conversion at different temperatures and bed materials in a batch fluidized bed reactor.

~ 45%). Even when the reactor was empty, almost half of the ethylene fed was converted at this temperature. This means that at a low temperature (850 °C), these oxygen carriers have a negligible catalytic effect on the removal of C_2H_4, which was

https://doi.org/10.1021/acs.energyfuels.3c02750
Energy Fuels 2023, 37, 16629−16638

only decomposed by thermal cracking, as was also revealed in a previous study using CH_4.[22]

On the contrary, the conversion of C_2H_4 was much improved when synthetic oxygen carriers were used. This indicates that the synthetic oxygen carriers have significant catalytic activity on the C_2H_4 conversion reactions (reforming, cracking, etc.) even at relatively low temperatures such as 850 °C.

As the temperature increased, C_2H_4 conversion by both noncatalytic (up to about 65% using sand at 950 °C) and catalytic reactions caused by the oxygen carriers increased. The observed catalytic effect of the low-cost oxygen carriers (ores and wastes) on ethylene conversion was quite similar for all low-cost materials, reaching conversions around 60 and 80% at 900 and 950 °C, respectively. Even so, when the synthetic oxygen carriers were used, the ethylene conversions were significantly higher, reaching values around 95% at 950 °C.

Among the synthetic oxygen carriers, Cu14Al_ICB achieved almost complete conversion of ethylene at the three temperatures. This could be attributed to the presence of metallic copper, Cu^0 (see Figure 4a), which was formed under typical high reduction conditions in BCLG operation.[11] As mentioned above, metallic compounds such as Cu^0 or Fe^0 can act as catalysts for hydrocarbon reforming.[32−34,44] Also, the catalytic activity of Cu14Al_ICB seems to be improved owing to its high porosity and BET specific surface area, which permitted a higher solid−gas contact. Formation of Fe^0 in most oxygen carriers was not possible due to thermodynamic limitations. Then, for Fe/Al oxygen carriers, the catalytic effect could not be attributed to the presence of Fe^0 since steam and CO_2 prevent the reduction to metallic iron (Figure 4a).[43] In spite of this, Fe/Al oxygen carriers showed a high ethylene conversion at all three temperatures. This higher conversion may be due in part to the catalytic effect of $FeAl_2O_4$ or Al_2O_3 but also to the relatively high specific surface area BET. As can be seen in Table 1, synthetic oxygen carriers had a much higher BET specific surface area than ores and wastes, which could improve solid−gas contact. It should be noted that the gas velocity used in the tests (about 20 cm/s) was high enough to avoid the influence on the results of small differences in the minimum fluidization velocities among the different oxygen carriers. The minimum fluidization velocities calculated for the oxygen carriers were: ilmenite (3.0−3.3 cm/s), iron ore (2.3−2.5 cm/s), iron sand (1.9−2.1 cm/s), LD Slag (1.8−1.9 cm/s), Fe10Al (1.4−1.5 cm/s), Fe20Al (1.6−1.7 cm/s), Fe25Al (1.7−1.9 cm/s), and Cu14Al (1.4−1.5 cm/s).

3.2.2. Benzene Conversion. The oxygen carrier used in BCLG can have a double effect on tar compounds as it can either oxidize the tars with the lattice oxygen or act as a catalyst for reforming or cracking reactions.[32] As gasification is performed under substoichiometric operating conditions, the limited presence of lattice oxygen can lead to incomplete tar and tar byproducts combustion. However, the catalytic effect of the oxygen carriers could be harnessed for tar removal by reforming or cracking reactions. Therefore, examining the isolated catalytic effect of the oxygen carriers on the removal of tar and tar byproducts is necessary for the proper selection of oxygen carriers for BCLG. In this work, benzene was used as a model compound to determine the catalytic effect of the oxygen carriers on the removal of tar byproducts. Figure 6 shows the conversion of benzene, X_{C6H6}, achieved during operation in the steady or pseudosteady state in the reduction period using different oxygen carriers at three temperatures.

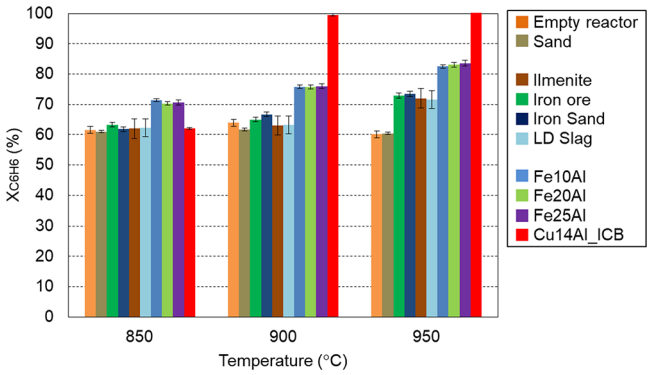

Figure 6. Benzene conversion at different temperatures and bed materials in a batch fluidized bed reactor.

Figure 6 shows that around 60% of the benzene fed was converted in the experiments carried out with the empty reactor or using sand as bed material at the three temperatures. This suggests that more than half of the benzene can be converted to low molecular weight products at temperatures equal to or higher than 850 °C without the need for any catalyst or bed materials. This is in line with the previous study carried out by Zhou et al.,[44] who reported that thermal cracking of benzene is possible at temperatures higher than 780 °C, despite the low yield. This behavior was different from that observed with the conversion of C_2H_4, which was an increasing function of temperature.

At 850 °C, similar conversions were found for wastes, ores, Cu14Al_ICB, and the inert material, indicating that the benzene was exclusively converted by noncatalytic reactions, such as thermal cracking. Only the Fe/Al oxygen carriers had a slight catalytic effect on benzene conversion at 850 °C. However, at higher working temperatures, such as 900 and 950 °C, catalytic reactions promoted benzene conversion, which varied among the different oxygen carrier materials. At 900 °C, the use of synthetic oxygen carriers caused an increase in benzene conversion, i.e., around 75% in the case of Fe/Al-based materials. On the other hand, the use of ores or wastes did not improve the benzene conversion compared to that when the reactor was empty and using a bed of sand.

At 950 °C, the use of ores and wastes slightly improved the benzene conversion by around 10% ($X_{C6H6} \sim 70\%$ with all ore- and waste-based materials) compared to that using sand and with the empty reactor. The use of Fe/Al synthetic oxygen carriers caused the benzene conversion to reach more than 80%, implying a sufficiently high catalytic activity of these materials at this temperature. The behavior of Cu14Al_ICB sets it apart from the other materials, as it promoted a complete benzene conversion at both 900 and 950 °C. This could be attributed to the formation of metallic copper, Cu^0, as stated in previous studies.[34] Also, in Table 1, it can be seen that Cu14Al_ICB presented a BET specific surface area of 79.4 m^2/g that could improve the oxygen carrier catalytic effect by promoting the gas−solid contact. Similarly, this could be a reason for the better benzene conversion for Fe/Al materials with respect to the ores and wastes. As shown in Table 1, the BET specific surface areas were much higher for the synthetic Fe/Al materials (19.7−60.9 m^2/g) compared to ores and wastes (<3 m^2/g). Likewise, the high particle porosity found in synthetic solids could be responsible for better gas diffusion inward.

https://doi.org/10.1021/acs.energyfuels.3c02750
Energy Fuels 2023, 37, 16629−16638

3.2.3. Methane Conversion. Despite its high energetic potential, CH_4 conversion into CO and H_2 is desired when the purpose of gasification is the production of syngas for further processing or transformation. However, previous studies carried out in BCLG units with continuous operation have reported the unwanted presence of methane in the fuel reactor outlet gas, with concentrations around 5−10 vol %.[6−16] This is likely due to the low reactivity of most of the oxygen carriers toward methane.[46,47] Steam reforming of methane is possible, but this reaction is slow, making necessary the use of catalysts.[32] In this section, the methane conversions obtained with the different oxygen carriers used in the batch fluidized bed are discussed.

Figure 7 shows the methane conversions achieved with the different solids at the three chosen temperatures in this study.

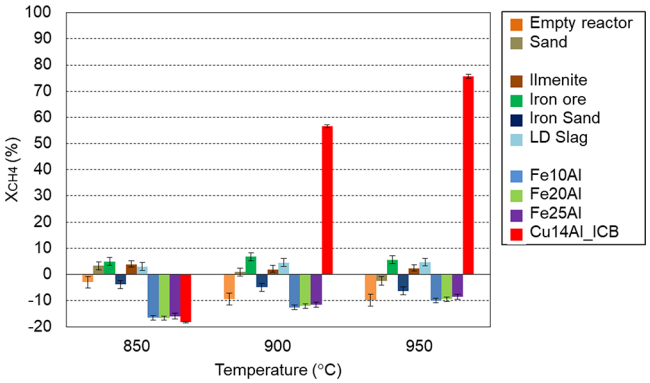

Figure 7. Methane conversion at different temperatures and bed materials in a batch fluidized bed reactor.

It can be seen that very low methane conversions or even methane generation (plotted as negative values) were obtained in most of the experiments. Using ores, wastes, and sand, methane conversion/generation values ranged from −10 to 10%, while using synthetic Fe/Al-based oxygen carriers, up to 17−18% of methane generation was achieved. This behavior does not agree with the results of a previous study where a methane conversion of 10−20% was achieved using sand as the bed but without feeding C_2H_4 and C_6H_6.[22] Therefore, the results observed indicate that CH_4 was generated in the present work as an intermediate compound in the decomposition of C_2H_4 and C_6H_6. This was in line with a previous study by Torres et al.,[26] which suggested that CH_4 was generated as an intermediate product of thermal cracking or hydrocracking of C_2H_4 and C_6H_6. This fact explains the different methane conversions achieved when different oxygen carriers were used since methane conversion was an increasing function of ethylene and benzene conversions.

Unlike the other oxygen carrier materials, Cu14Al_ICB showed a clear catalytic effect on methane reforming, reaching conversions of 57 and 76% at 900 and 950 °C, respectively. In fact, during a series of experiments carried out at eight different temperatures between 750 and 950 °C, it was found that the catalytic effect of Cu14Al_ICB in the hydrocarbon reforming reaction increased exponentially from 880 to 890 °C.

Figure 8 shows the screening of ethylene, benzene, and methane conversion using Cu14Al_ICB in the fluidized bed reactor. It can be seen that the increase in temperature from 880 to 890 °C promoted a sharp change in the intensification

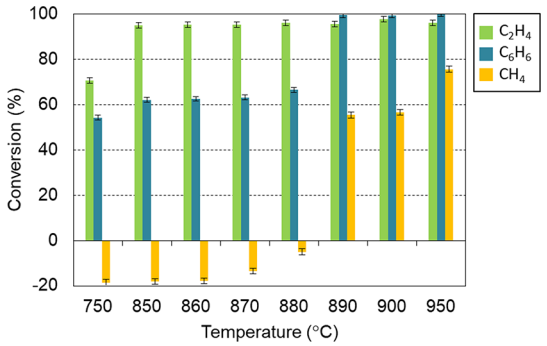

Figure 8. C_2H_4, C_6H_6, and CH_4 conversions at different temperatures using the Cu14Al_ICB solid.

of CH_4 and C_6H_6 conversions, whereas C_2H_4 remained almost stable.

3.3. Comparison of Benzene Conversion with Tar Byproduct Emissions in BCLG Prototypes. In order to determine the validity of the method used in this work to evaluate the catalytic effect of oxygen carriers in tar byproduct removal for BCLG application, the benzene conversions obtained in the batch fluidized bed reactor were compared with available tar byproduct concentration data from previous studies on a 1.5 kW_{th} BCLG prototype with continuous biomass feed.[6−12] Figure 9 shows the relationship between the benzene conversions obtained in this work and the tar byproduct concentrations measured in the 1.5 kW_{th} ICB-CSIC prototype working with the same oxygen carriers and at very similar temperatures. All the experiments in the continuous unit were carried out at an oxygen-to-fuel ratio ∼0.3, which means the transfer to the fuel of 0.3 mol/h of O per each mol/h of O needed for complete combustion of the biomass fed.

It can be seen that when high benzene conversions were reached in the batch fluidized bed reactor, low tar byproduct concentrations were measured in the syngas generated in the BCLG prototype working with the continuous feeding of biomass. Hence, this establishes a relationship between the results obtained in the batch fluidized bed reactor and those found in the prototype. Likewise, the temperature largely determined the tar byproduct conversion in both types of reactors. The experiments carried out at high temperature (950 °C) in the batch fluidized bed reactor showed benzene conversions higher than 70 and 80% when using low-cost and synthetic oxygen carriers, respectively. On the other hand, the tar byproduct concentrations in most experiments carried out in the 1.5 kW_{th} BCLG unit at a similar temperature were less than 3.0 g/kg dry biomass and 2.0 g/kg dry biomass when low-cost materials and synthetic oxygen carriers were used, respectively. At temperatures of 850 and 900 °C, benzene conversions in the batch reactor were between ∼60 and ∼75% and tar byproduct concentrations in the 1.5 kW_{th} BCLG unit between 2.5 and 4.5 g/kg. Exceptionally, the use of the Cu14Al_ICB oxygen carrier reached tar byproduct values lower than 2 g/kg at 900 °C. This corroborated the exponential increase of catalytic activity of the Cu-based oxygen carrier when the temperature increased from 850 to 900 °C. Apart from the significant effect the reaction temperature had on both benzene conversions in the batch fluidized bed reactor and tar byproduct concentration in syngas from the 1.5 kW_{th} unit, the nature of the oxygen carriers was also important. The results between the two different reactor

https://doi.org/10.1021/acs.energyfuels.3c02750
Energy Fuels 2023, 37, 16629−16638

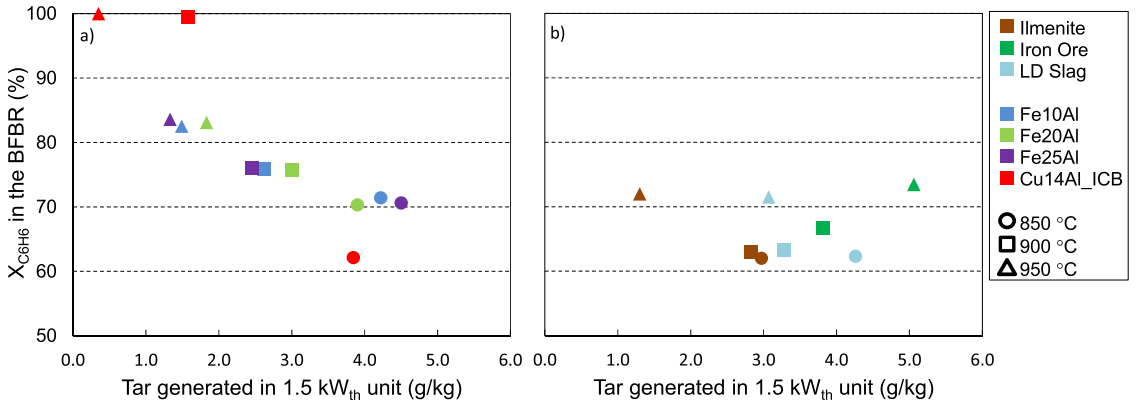

Figure 9. Relationship between benzene conversions in the batch fluidized bed reactor (BFBR) and tar emissions in the 1.5 kW_{th} continuous BCLG unit (oxygen-to-fuel ratio ~ 0.3). (a) Synthetic oxygen carriers and (b) ore- and waste-based materials.

systems are in line, showing that tar byproduct removal is higher when using synthetic oxygen carriers rather than the low-cost ones.

It can be concluded that the method used to analyze the catalytic effect of the oxygen carrier on benzene conversion is useful to infer the behavior of the oxygen carrier for tar byproduct removal in BCLG continuous units. Still, even at the same temperatures, the relationship between the results of the batch reactor and the continuous unit must be interpreted separately for each oxygen carrier since each one presents different catalytic activities. Furthermore, it must be considered that in a continuous operation, the oxygen carrier enters the fuel reactor in a partially oxidized manner, which can result in partial tar or tar byproduct removal due to possible combustion or partial combustion.[48,49] However, it is expected that due to the low reactivity of the oxygen carriers with tars and hydrocarbons (even with methane as seen above), most of the lattice oxygen will be consumed in the combustion of H_2 and CO and its contribution to the combustion of tars and hydrocarbons will be minimal. Therefore, reforming and cracking reactions should be the main cause of tar and tar byproduct removal when operating in a BCLG continuous unit.

4. CONCLUSIONS

The catalytic effect on the conversion of C_2H_4 and C_6H_6 of different low-cost and synthetic oxygen carriers suitable for the BCLG process was evaluated in a batch fluidized bed reactor at 850, 900, and 950 °C. The results suggest that the ores and wastes used had a low catalytic effect on the conversion of ethylene and benzene. However, the conversion increased with increasing temperature. Depending on the temperature, the ethylene and benzene conversions achieved were 40−80% and 60−70%, respectively, but most of the conversion was attributed to the noncatalytic thermal cracking reactions. In contrast, the Fe/Al-based synthetic oxygen carriers improved the ethylene and benzene conversions up to 82−92% and 75−82%, respectively. The Cu-based synthetic oxygen carrier (Cu14Al_ICB) showed the highest catalytic effect on the conversion of ethylene and benzene, reaching almost complete conversions for both compounds at temperatures of >900 °C. In all cases, the catalytic effect on the conversion of ethylene and benzene increased with temperature.

Methane was generated as an intermediate compound from ethylene and benzene conversion. Cu14Al_ICB was the only oxygen carrier that showed a significantly high methane conversion, reaching around 55 and 75% at 900 and 950 °C, respectively.

A qualitative relationship between the benzene conversion achieved in the batch fluidized bed reactor and the tar byproduct concentrations measured in the syngas generated in a 1.5 kW_{th} BCLG prototype working in continuous operation was observed. The higher the benzene conversion in the fluidized bed reactor, the lower the tar byproduct concentrations measured in the syngas generated in the prototype.

AUTHOR INFORMATION

Corresponding Author

Francisco García-Labiano − *Instituto de Carboquímica, Consejo Superior de Investigaciones Científicas (ICB-CSIC), 50018 Zaragoza, Spain;* orcid.org/0000-0002-5857-0976; Email: glabiano@icb.csic.es

Authors

Iván Samprón − *Instituto de Carboquímica, Consejo Superior de Investigaciones Científicas (ICB-CSIC), 50018 Zaragoza, Spain;* orcid.org/0000-0002-8372-6151

Victor Purnomo − *Department of Chemistry and Chemical Engineering, Chalmers University of Technology, 412 58 Göteborg, Sweden;* orcid.org/0000-0001-6289-9603

Tobias Mattisson − *Department of Space, Earth, and Environment, Chalmers University of Technology, 412 58 Göteborg, Sweden;* orcid.org/0000-0003-3942-7434

Henrik Leion − *Department of Chemistry and Chemical Engineering, Chalmers University of Technology, 412 58 Göteborg, Sweden*

Luis F. de Diego − *Instituto de Carboquímica, Consejo Superior de Investigaciones Científicas (ICB-CSIC), 50018 Zaragoza, Spain;* orcid.org/0000-0002-4106-3441

Complete contact information is available at: https://pubs.acs.org/10.1021/acs.energyfuels.3c02750

Notes

The authors declare no competing financial interest.

ACKNOWLEDGMENTS

This work was supported by the CO2SPLIT project, Grant PID2020-113131RB-I00, funded by MICIN/AEI/10.13039/501100011033. I.S. thanks the Spanish Ministerio de Ciencia,

Innovación y Universidades (MICIU) for the PRE2018-086217 predoctoral fellowship.

REFERENCES

(1) Mendiara, T.; García-Labiano, F.; Abad, A.; Gayán, P.; de Diego, L. F.; Izquierdo, M. T.; Adánez, J. Negative CO_2 emissions through the use of biofuels in chemical looping technology: A review. *App. Energy* **2018**, *232*, 657−684.

(2) Sikawar, V. S.; Zhao, M.; Fennell, P. S.; Shah, N.; Anthony, E. J. Progress in biofuel production from gasification. *Prog. Energy Combust. Sci.* **2017**, *61*, 189−248.

(3) Lyngfelt, A. Chemical Looping Combustion: Status and Development Challenges. *Energy Fuels* **2020**, *38* (8), 9077−9093.

(4) Adánez, J.; Abad, A.; Mendiara, T.; Gayán, P.; de Diego, L. F.; García-Labiano, F. Chemical looping combustion of solid fuels. *Prog. Energ Combust* **2018**, *65*, 6−66.

(5) Lin, Y.; Wang, H.; Wang, Y.; Huo, R.; Huang, Z.; Liu, M.; et al. Review of Biomass Chemical Looping Gasification in China. *Energy Fuels* **2020**, *34* (7), 7847−7862.

(6) Condori, O.; García-Labiano, F.; de Diego, L. F.; Izquierdo, M. T.; Abad, A.; Adánez, J. Biomass chemical looping gasification for syngas production using ilmenite as oxygen carrier in a 1.5 kWth unit. *Chem. Eng. J.* **2021**, *405*, No. 126679.

(7) Samprón, I.; de Diego, L. F.; García-Labiano, F.; Izquierdo, M. T.; Abad, A.; Adánez, J. Biomass Chemical Looping Gasification of pine Wood using a synthetic Fe_2O_3/Al_2O_3 oxygen carrier in a continuous unit. *Bioresour. Technol.* **2020**, *316*, No. 123908.

(8) Condori, O.; García-Labiano, F.; de Diego, L. F.; Izquierdo, M. T.; Abad, A.; Adánez, J. Biomass chemical looping gasification for syngas production using LD Slag as oxygen carrier in a 1.5 kWth unit. *Fuel Process. Technol.* **2021**, *222*, No. 106963.

(9) Condori, O.; de Diego, L. F.; García-Labiano, F.; Izquierdo, M. T.; Abad, A.; Adánez, J. Syngas production in a 1.5 kWth biomass chemical looping gasification unit using Fe and Mn ores as the oxygen carrier. *Energy Fuels* **2021**, *35* (21), 17182−17196.

(10) Samprón, I.; de Diego, L. F.; García-Labiano, F.; Izquierdo, M. T. Effect of the Fe content on the behavior of synthetic oxygen carriers in a 1.5 kW biomass chemical looping gasification unit. *Fuel* **2022**, *309*, No. 122193.

(11) Sampron, I.; Cabello, A.; García-Labiano, F.; Izquierdo, M. T.; de Diego, L. F. An innovative Cu-Al oxygen carrier for the biomass chemical looping gasification process. *Chem. Eng. Jour* **2023**, *465*, No. 142919.

(12) Condori, O.; Abad, A.; Izquierdo, M. T.; de Diego, L. F.; García-Labiano, F.; Adánez, J. Assessment of the chemical looping gasification of wheat straw pellets at the 20 kWth scale. *Fuel* **2023**, *344*, No. 128059.

(13) Wei, G.; He, F.; Huang, Z.; Zheng, A.; Zhao, K.; Li, H. Continuous Operation of a 10 kWth Chemical Looping Integrated Fluidized Bed Reactor for Gasifying Biomass Using an Iron-Based Oxygen Carrier. *Energy Fuels* **2015**, *29* (1), 233−241.

(14) Wei, G.; He, F.; Zhao, Z.; Huang, Z.; Zheng, A.; Zhao, K.; et al. Performance of Fe-Ni bimetallic oxygen carriers for chemical looping gasification of biomass in a 10 kWth interconnected circulating fluidised bed reactor. *Int. J. Hydrog Energy* **2015**, *40*, 16021−16032.

(15) Huseyin, S.; Wei, G.-Q.; Li, H.-B.; He, F.; Huang, Z. Chemical-looping gasification of biomass in a 10 kWth interconnected fluidized bed reactor using Fe_2O_3/Al_2O_3 oxygen carrier. *J. Fuel Chem. Technol.* **2014**, *42* (8), 922−931.

(16) Ge, H.; Guo, W.; Shen, L.; Song, T.; Xiao, J. Biomass gasification using chemical looping in a 25 kWth reactor with natural hematite as oxygen carrier. *Chem. Eng. J.* **2016**, *286*, 174−183.

(17) Purnomo, V.; Yilmaz, D.; Leion, H.; Mattison, T. Study of defluidization of iron- and manganese-based oxygen carriers under highly reducing conditions in a lab-scale fluidized-bed batch reactor. *Fuel Process. Technol.* **2021**, *219*, No. 106687.

(18) Purnomo, V.; Mei, D.; Soleimanisalim, A. H.; Mattisson, T.; Leion, H. Effect of the Mass Conversion Degree of an Oxygen Carrier on Char Conversion and Its Implication for Chemical Looping Gasification. *Energy Fuels* **2022**, *36* (17), 9768−9779.

(19) Hildor, F.; Soleimanisalim, A. H.; Seeman, M.; Mattisson, T.; Leion, H. Tar characteristics generated from a 10 kWth chemical-looping biomass gasifier using steel converter slag as an oxygen carrier. *Fuel* **2023**, *331*, No. 125770.

(20) Tian, X.; Niu, P.; Ma, Y.; Zhao, H. Chemical-looping gasification of biomass: Part II Tar yields and distribution. *Biomass Bioenerg* **2018**, *108*, 178−189.

(21) Sampron, I.; de Diego, L. F.; García-Labiano, F.; Izquierdo, M. T. Optimization of synthesis gas production in the biomass chemical looping gasification process operating under auto-thermal conditions. *Energy* **2021**, *26*, No. 120317.

(22) Sampron, I.; de Diego, L. F.; García-Labiano, F.; Izquierdo, M. T.; Adánez, J. Influence of an Oxygen Carrier on the CH4 Reforming Reaction Linked to the Biomass Chemical Looping Gasification Process. *Energy Fuels* **2022**, *36* (17), 9460−9469.

(23) Woolcock, P. J.; Brown, R. C. A review of cleaning technologies for biomass-derived syngas. *Biomass Bionerg* **2013**, *52*, 54−84.

(24) Devi, L.; Ptasinski, K. J.; Janssen, F. J. A review of the primary measures for tar elimination in biomass gasification processes. *Biomass Bioenergy* **2003**, *24* (2), 125−140.

(25) Guan, G.; Kaewpanha, M.; Hao, X.; Abudula, A. Catalytic reforming of tar and volatiles from walnut shell pyrolysis over a novel Ni/olivine/La2O3 supported on ZrO2. *Renewable Sustainable Energy Rev.* **2016**, *58*, 450−461.

(26) Torres, W.; Pansare, S. S.; Goodwin, J. G., Jr Hot gas removal of tars, ammonia, and hydrogen sulfide from biomass gasification gas. *Catal. Rev.* **2007**, *49*, 407−456.

(27) Kinoshita, C. M.; Wang, Y.; Zhou, J. Tar formation under different gasification conditions. *J. Anal. Appl. Pyrolysis* **1994**, *29*, 169−181.

(28) Elliott, D. C. Relation of reaction time and temperature to chemical composition of pyrolysis oils. *ACS Symp. Ser.* **1988**, *376*, 55−65.

(29) Tregrossi, A.; Ciajolo, A.; Barbella, R. The combustion of benzene in rich premixed flames at atmospheric pressure. *Combust. Flame* **1999**, *117*, 553−561.

(30) Han, J.; Kim, H. The reduction and control technology of tar during biomass gasification/pyrolysis: an overview. *Renewable Sustainable Energy Rev.* **2008**, *12*, 397−416.

(31) Narvaez, I.; Corella, J.; Orío, A. Fresh Tar (from a Biomass Gasifier) Elimination over a Commercial Steam-Reforming Catalyst. Kinetics and Effect of Different Variables of Operation. *Ind. Eng. Chem. Res.* **1997**, *36*, 317−327.

(32) Cortazar, M.; Santamaria, L.; Lopez, G.; Alvarez, J.; Zhang, L.; Wang, R.; Bi, X.; Olazar, M. A comprhensive review of primary strategies for tar removal in biomass gasification. *Energy Convers. Manage.* **2023**, *276*, No. 116496.

(33) Virginie, M.; Adánez, J.; Courson, C.; de Diego, L. F.; García-Labiano, F.; Niznansky, D.; Kiennemann, A.; Gayán, P.; Abad, A. Effect of Fe−olivine on the tar content during biomass gasification in a dual fluidized bed. *Appl. Catal., B* **2012**, *121*−*122*, 214−222.

(34) Zeng, J.; Hu, J.; Qiu, Y.; Zhang, S.; Zeng, D.; Xiao, R. Multi-function of oxygen carrier for in-situ tar removal in chemical looping gasification: Naphthalene as model compound. *Appl. Energy* **2019**, *253*, No. 113502.

(35) Keller, M.; Leion, H.; Mattisson, T.; Thunman, H. Investigation of Natural and Synthetic Bed Materials for Their Utilization in Chemical Looping Reforming for Tar Elimination in Biomass-Derived Gasification Gas. *Energy Fuels* **2014**, *28*, 3833−3840.

(36) Keller, M.; Leion, H.; Mattisson, T. Chemical looping tar reforming using La/Sr/Fe-containing mixed oxides supported on ZrO_2. *Appl. Catal., B* **2016**, *183*, 298−307.

(37) Bain, R.; Magrini-Bair, K.; Hensley, J.; Jablonski, W.; Smith, K.; Gaston, K.; Yung, M. Pilot scale production of mixed alcohols from wood. *Ind. Eng. Res.* **2014**, *53* (6), 2204−2218.

https://doi.org/10.1021/acs.energyfuels.3c02750
Energy Fuels 2023, 37, 16629−16638

(38) Leion, H.; Frick, V.; Hildor, F. Experimental Method and Setup for Laboratory Fluidized Bed Reactor Testing. *Energies* **2018**, *11* (10), 2505.
(39) Purnomo, V.; Staničić, I.; Mei, D.; Soleimanisalim, A. H.; Mattisson, T.; Rydén, M.; Leion, H. Performance of iron sand as an oxygen carrier at high reduction degrees and its potential use for chemical looping gasification. *Fuel* **2023**, *339*, No. 127310.
(40) Hildor, F.; Leion, H.; Linderholm, C. J.; Mattisson, T. Steel converter slag as an oxygen carrier for chemical-looping gasification. *Fuel Pro Tech* **2020**, *210*, No. 106576.
(41) de Diego, L. F.; Gayán, P.; García-Labiano, F.; Celaya, J.; Abad, A.; Adánez, J. Impregnated CuO/Al_2O_3 Oxygen Carriers for Chemical-Looping Combustion: Avoiding Fluidized Bed Agglomeration. *Energy Fuels* **2005**, *19* (5), 1850−1856.
(42) Abad, A.; García-Labiano, F.; de Diego, L. F.; Gayán, P.; Adánez, J. Reduction Kinetics of Cu-, Ni-, and Fe-Based Oxygen Carriers Using Syngas ($CO + H_2$) for Chemical-Looping Combustion. *Energy Fuels* **2007**, *21*, 1843−1853.
(43) Cabello, A.; Abad, A.; García-Labiano, F.; Gayán, P.; de Diego, L. F.; Adánez, J. Kinetic determination of a highly reactive impregnated Fe_2O_3/Al_2O_3 oxygen carrier for use in gas-fueled Chemical Looping Combustion. *Chem. Eng. J.* **2014**, *258*, 265−280.
(44) Zhou, Z.; Deng, G.; Li, L.; Liu, X.; Sun, Z.; Duan, L. Chemical looping co-conversion of CH_4 and CO_2 using Fe_2O_3/Al_2O_3 pellets as both oxygen carrier and catalyst in a fluidized bed reactor. *Chem. Eng. J.* **2022**, *428*, No. 132133.
(45) Zhou, H.; Gao, X.; Liu, P.; Zhu, Q.; Wang, J.; Li, X. An experimental and simulated investigation on pyrolysis of blended cyclohexane and benzene under supercritical pressure. *Pet. Chem.* **2017**, *57*, 71−78.
(46) Abad, A.; Adánez, J.; García-Labiano, F.; de Diego, L. F.; Gayán, P.; Celaya, J. Mapping of the range of operational conditions for Cu-, Fe-, and Ni-based oxygen carriers in chemical-looping combustion. *Chem. Eng. Sci.* **2007**, *62*, 533−549.
(47) Mendiara, T.; Abad, A.; de Diego, L. F.; García-Labiano, F.; Gayán, P.; Adánez, J. Reduction and oxidation kinetics of Tierga iron ore for Chemical Looping Combustion with diverse fuels. *Chem. Eng. J.* **2019**, *359*, 37−46.
(48) Dieringer, P.; Marx, F.; Alobaid, F.; Ströle, J.; Epple, B. Process Control Strategies in Chemical Looping Gasification-A novel Process for the Production of Biofuels Allowing for Net Negative CO_2 Emissions. *Appl. Sci.* **2020**, *10*, 4271.
(49) Dieringer, P.; Marx, F.; Michel, B.; Ströhle, J.; Epple, B. Design and control concept of a 1 MWth chemical looping gasifier allowing for efficient autothermal syngas production. *Int. J. Greenhouse Gas Control* **2023**, *127*, No. 103929.

https://doi.org/10.1021/acs.energyfuels.3c02750
Energy Fuels 2023, 37, 16629−16638